

This is author version of article published as:

Frost, Ray L. and Cejka, Jiri and Ayoko, Godwin A. and Weier, Matt L. (2007) Raman spectroscopic and SEM analysis of sodium zippeite . *Journal of Raman Spectroscopy* 38(10):pp. 1311-1319.

Copyright 2007 John Wiley & Sons

Raman spectroscopic and SEM analysis of sodium zippeite

Ray L. Frost^{1*}, Jiří Čejka^{1,2}, Godwin A. Ayoko¹ and Matt L. Weier¹

1. Inorganic Materials Research Program, School of Physical and Chemical Sciences, Queensland University of Technology, GPO Box 2434, Brisbane, Queensland 4001, Australia.
2. National Museum, Václavské náměstí 68, 115 79 Praha 1, Czech Republic.

Abstract

Raman at 298 and 77 K and infrared spectra of two samples of sodium-zippeite were studied and interpreted. U-O bond lengths in uranyl were calculated and compared with those inferred from the X-ray single crystal structure data of a synthetic sodium-zippeite analog. Hydrogen-bonding network in the studied samples is discussed. O-H...O bond lengths were calculated and compared with those predicted from the X-ray single crystal structure analysis.

Key words: sodium-zippeite, uranyl mineral, Raman and infrared spectroscopy, U-O bond lengths in uranyl, hydrogen-bonding network

Introduction

Uranyl sulfates of the zippeite group are common constituents in the oxidized zone of uranium deposits^{1,2}. Zippeites may impact upon the mobility of uranium and heavy metals in mine tailings and may form in a geological repository for nuclear waste such as results from spent nuclear fuel. Uranyl sulfates may determine the mobility and fate of uranium in natural systems. These uranyl sulfates are also important as alteration products of nuclear waste. They may incorporate radionuclides into their crystal structure, thus impacting the mobility of some radionuclides². Uranyl sulfate minerals are not abundant, however, they are widespread, occurring in uranium deposits worldwide. The uranyl sulfate minerals including zippeites originate and are formed as a result of the oxidation of sulfide minerals connected with the formation of sulfate anions in the presence of hexavalent uranium in the form of uranyl ions, $(\text{UO}_2)^{2+}$ ².

Uranyl minerals of the zippeite-group have been poorly-defined for many years³⁻⁵. Very few spectroscopic studies have been undertaken even though Raman spectroscopy has been applied to other minerals containing the uranyl group⁶⁻¹¹. It is presumed that the zippeite minerals are simple hydrated uranyl sulfates. Frondel and Weeks first showed that these minerals are not simple hydrated uranyl sulfates, but in fact each contain a cation in addition to the uranyl ion⁴. Description and comparison of natural samples with their synthetic

analogues were published in 1976 by Frondel et al.⁵. Chemical composition, refractive indices and X-ray powder patterns were included in this paper. However, some confusions in these results were observed. O'Brien and Williams¹² and Haacke and Williams¹³ presented ΔG°_f values for synthetic K-, (NH₄)-, Na-, Mg-, Ni-, Co- and Zn-zippeites and assumed extensive solid solution formation between divalent cation containing zippeites, between K- and (NH₄)-zippeites, but not between K- and Na-zippeites. Extensive crystallochemical and structural study of synthetic zippeites was recently published by Burns et al.¹⁴ followed by a dissertation describing in detail some natural zippeites². Both authors found the layered zippeites are topologically identical. The sheet contains zig-zag chains of edge-sharing uranyl pentagonal dipyramids, and the chains are connected by the sharing of vertices between the uranyl pentagonal dipyramids and sulfate tetrahedra. Each sulfate tetrahedron is linked to four different uranyl dipyramids¹⁵. The sheet is made up of chains of uranyl pentagonal dipyramids that are two polyhedra wide. The chains are crosslinked through (SO₄)²⁻ tetrahedra, resulting in uranyl sulfate sheets. The composition of the sheet is dependant upon the distribution of (O²⁻)/(OH)⁻ in each zippeite phase². The uranyl sulfate sheets are in some cases (e.g. Mg-, Zn-, Co-, (NH₄)-zippeites) anhydrous, [(UO₂)₂(SO₂)O₂], or oxy anions may be partly substituted by hydroxyls e. g. in zippeite (the name zippeite proposed by Frondel for K-zippeite from Jáchymov, studied by Nováček in 1935⁵, [(UO₂)₄(SO₄)₂O₃(OH)]), or in sodium-zippeite, [(UO₂)₄(SO₄)₄O₅(OH)₃]^{14,15}. Burns et al.¹⁴ concluded that the distribution of interlayer constituents, i. e. mono- and divalent cations and water molecules can be rationalized on the basis of the bonding requirements of the uranyl sulfate sheets¹⁵. It may be assumed that the (UO₂)/(SO₄)²⁻ molar ratio in the layers is probably close to 2 with some variability in the O/OH ratio. However, McCollam² proved that practically in all analysed natural zippeites the molar ratio $M^+(M^{2+})/(UO_2)^{2+}/(SO_4)^{2-}$ was lower than expected from the stoichiometry. The interlayer is open and able to include monovalent and divalent cations for balancing the charge of the layers together with water molecules. Hydrogen-bonding network plays also an important role for the origin and stability of zippeites.

Frondel et al.⁵ attributed to natural and synthetic sodium-zippeite the formula Na₄[(UO₂)₆(SO₄)₃(OH)₁₀]. 4H₂O. According to Burns et al.¹⁴, the formula for synthetic sodium-zippeite is Na₅(H₂O)₁₂[(UO₂)₈(SO₄)₄O₅(OH)₃] with Z = 4, 8 symmetrically distinct U⁶⁺ atoms (one UO₂O₅, five UO₂O₄(OH) and two UO₂O₃(OH)₂) and four symmetrically distinct S⁶⁺ atoms. Each (OH)⁻ group is bonded to two U⁶⁺ cations, and is located at a common equatorial vertex. In Na-zippeite, there are three symmetrically distinct (OH)⁻ groups, two of which occur along a shared edge between uranyl pentagonal dipyramids¹⁴. The presence of some U_x(O,OH)_y groupings was assumed and proved in the crystal structure of synthetic Na-zippeite. In the interlayer, Na cations are coordinated by six or seven ligands (O_{uranyl} atoms and/or O_{U-S} atoms and/or water molecules). Five Na cations and twelve water molecules form a complex interlayer in synthetic Na-zippeite. Eight water molecules are shared between two Na⁺ cations and four are bonded to only one Na⁺ cation. The interlayer of the synthetic Na-zippeite contains also a substantial number of hydrogen bonds thus forming a complex hydrogen-bonding network¹⁴.

It has been shown that the uranyl sulfate sheet topology is very similar in all zippeite-type minerals and their synthetic analogues^{14,16,17}. However, the relatively large interlayer enables complex localization of monovalent and/or divalent cations and the formation of solid solutions, and of water molecules. Water molecules may be coordinated by cations or only hydrogen bonded. McCollam² assumes possible existence of solid solutions of zippeites containing monovalent cations Na⁺, K⁺ and (NH₄)⁺, and may also contain divalent cations.

Water molecules from the interlayer and hydroxyls in the sheets participate in formation of a very complex hydrogen-bonding network in Na-zippeite¹⁴.

Sodium-zippeite was described from Jáchymov, Czech Republic¹⁸, Geevor mine, St. Just, Cornwall, England¹⁹ Rožná, Czech Republic²⁰ La Creusaz uranium prospect, Switzerland²¹, Jánská žíla, Březové Hory, Příbram, Czech Republic²². Infrared spectra and thermal analysis of natural and synthetic zippeites were reviewed by Čejka²³. Raman spectroscopy has proven very useful for the study of minerals²⁴⁻²⁶. Indeed Raman spectroscopy has proven most useful for the study of diagenetically related minerals as often occurs with uranyl secondary minerals^{7-10,27}. Some previous studies have been undertaken by the authors using Raman spectroscopy to study complex secondary minerals formed by crystallisation from concentrated sulphate solutions²⁸. The aim of this paper is to present Raman and infrared spectra of natural sodium-zippeite and to discuss the spectra from the structural point of view. The paper is a part of systematic studies of vibrational spectra of minerals of secondary origin in the oxide supergene zone and their synthetic analogs.

Experiments

Minerals

The Na-zippeite minerals used in this work were obtained from the Mineralogical research Company and originated from The Happy Jack Mine, White Canyon District, San Juan County, USA. The mineral was analysed by EDX for chemical composition and by powder X-ray diffraction for phase identification.

SEM and X-ray microanalysis

Zippeite samples were coated with a thin layer of evaporated carbon and secondary electron images were obtained using an FEI Quanta 200 scanning electron microscope (SEM). For X-ray microanalysis (EDX), three samples were embedded in Araldite resin and polished with diamond paste on Lamplan 450 polishing cloth using water as a lubricant. The samples were coated with a thin layer of evaporated carbon for conduction and examined in a JEOL 840A analytical SEM at 25kV accelerating voltage. Preliminary analyses of the zippeite samples were carried out on the FEI Quanta SEM using an EDAX microanalyser, and microanalysis of the clusters of fine crystals was carried out using a full standards quantitative procedure on the JEOL 840 SEM using a Moran Scientific microanalysis system. Uranium oxide was used as a standard for U. The K-K α peak is strongly overlapped by the U-M lines and was deconvolved using a peak strip routine, which gave similar results to a peak fit routine used by the EDAX analysis software. However some uncertainty remains in the quantitative measurements of K in the presence of U. Oxygen was not measured directly but was calculated using assumed stoichiometries to the other elements analysed.

Raman spectroscopy

Crystals of the sodium zippeite were placed on the stage of an Olympus BHSM microscope, equipped with 10x and 50x objectives and part of a Renishaw 1000 Raman microscope system, which also includes a monochromator, a filter system and a Charge Coupled Device (CCD). Raman spectra were excited by a HeNe laser (633 nm) at a resolution of 2 cm⁻¹ in the range between 100 and 4000 cm⁻¹. Repeated acquisition using the highest magnification was accumulated to improve the signal to noise ratio. Spectra were calibrated

using the 520.5 cm^{-1} line of a silicon wafer. In order to ensure that the correct spectra are obtained, the incident excitation radiation was scrambled. Previous studies by the authors provide more details of the experimental technique. Spectra at liquid nitrogen temperature were obtained using a Linkam thermal stage (Scientific Instruments Ltd, Waterfield, Surrey, England). Details of the technique have been published by the authors²⁹⁻³².

Infrared Spectroscopy

Infrared spectra were obtained using a Nicolet Nexus 870 FTIR spectrometer with a smart endurance single bounce diamond ATR cell. Spectra over the $4000\text{--}525\text{ cm}^{-1}$ range were obtained by the co-addition of 64 scans with a resolution of 4 cm^{-1} and a mirror velocity of 0.6329 cm/s . Spectral manipulation such as baseline adjustment, smoothing and normalisation was performed using the GRAMS® software package (Galactic Industries Corporation, Salem, NH, USA).

Results and discussion

Scanning Electron Microscopy

The SEM image of the Na zippeite studied in this work is shown in Figures 1. The numbers on the image show the points where EDX analyses were undertaken. Figure 1 shows a mass of crystals agglomerated together. The crystals appear to have been formed in solution as a colloid and possibly because of electrostatic attraction have assembled into a crystalline mass. The agglomerated crystals are $> 5\text{ }\mu\text{m}$ in length. Figure 1 shows the close relationship between different single crystals and several edge to face and face to face stacking may be observed. Such stacking supports the concept of electrostatic attraction between the particles. Figure 1 seems to show the particles have been damaged through some mechanochemical treatment such as a tumbling action. Many of the crystals are large and greater than $10\text{ }\mu\text{m}$. SEM images reveal that the zippeite morphology consists of an array of rosettes of flat elongated crystals. The rosettes may be up to $50\text{ }\mu\text{m}$ in diameter while individual crystals are up to $20\text{ }\mu\text{m}$ in length and less than $0.5\text{ }\mu\text{m}$ in thickness.

The results of the EDX analyses of the zippeite are reported in Table 1. The analyses are taken from different crystals. The presence of carbon results from the coating of the sample. The zippeite from The Happy Jack Mine are based upon sodium as the monovalent cation. Thus the formula of the zippeite samples studied is close to that for synthetic Na-zippeite by Burns et al.¹⁴. In Dana's new mineralogy and Anthony's Handbook, a number of zippeites are characterised. One of the minerals among others from The Happy Jack Mine is a sodium zippeite. Both report the Na-zippeite to be orthorhombic³³. It is noted that a synthetic sodium-zippeite as prepared by Burns¹⁴, $\text{Na}_5(\text{H}_2\text{O})_{12}[(\text{UO}_2)_8(\text{SO}_4)_4\text{O}_5(\text{OH})_3]$, was monoclinic, $P2_1/a$, $a\ 17.6425(110)$, $b\ 14.6272(9)$, $c\ 17.6922(11)\text{ }\text{\AA}$, $\beta\ 104.461(1)^\circ$, $Z = 4$.

Raman and Infrared Spectroscopy

In the crystal structure of synthetic Na zippeite, there are present four symmetrically distinct S^{6+} [as $(\text{SO}_4)^{2-}$ units]. Because of the Td symmetry lowering, all $(\text{SO}_4)^{2-}$ vibrations may be infrared and Raman active, and the doubly degenerate ν_2 $(\text{SO}_4)^{2-}$ bending vibrations, the triply degenerate antisymmetric stretching vibrations ν_3 $(\text{SO}_4)^{2-}$ and the triply degenerate

bending vibrations ν_4 (SO_4)²⁻ split. Raman and infrared bands assigned to the ν_3 (SO_4)²⁻ are located in the region 1280-1040 cm^{-1} , bands attributed to the ν_1 symmetric stretching vibrations (SO_4)²⁻ in 1020-950 cm^{-1} , and bands assigned to the ν_4 (SO_4)²⁻ and ν_2 (SO_4)²⁻ bending vibration in 680-560 cm^{-1} and 560-350 cm^{-1} , respectively. As in the case of the (UO_2)²⁺ stretching vibrations, some overlap or coincidence of the (SO_4)²⁻ stretching vibrations and δ U-OH bending is possible. Bands connected with libration modes of water molecules may coincide especially with bands attributed to the (SO_4)²⁻ bending vibrations.

The Raman spectra in the 950 to 1050 cm^{-1} region of two mineral samples from the happy Jack Mine are shown in Figure 2. The reason for showing the spectra of two samples is to prove consistency of measurement. An intense band at 1009.5 cm^{-1} in the 298 K spectrum which shifts to 1011.6 cm^{-1} in the 77 K spectrum is attributed to the SO_4^{2-} symmetric stretching vibration. The bands are asymmetric on the lower wavenumber side and an additional band in the 1006-7 cm^{-1} position is observed. A single band was observed for uranopilite at around 1008.7 cm^{-1} in the 298 K spectrum and at 1008.9 cm^{-1} in the 77 K spectrum and is assigned to the SO_4^{2-} symmetric stretching vibration^{6-11,28}. The band shows a slight shift to higher wavenumbers upon cooling to 77 K. The infrared spectra of zippeite is shown in Figure 3. A number of overlapping infrared bands are observed at 1173, 1140, 1100, 1069 and 1051 cm^{-1} . A low intensity band is observed at \sim 1015 cm^{-1} and is assigned to the infrared activated SO_4^{2-} symmetric stretching vibration.

The infrared spectra of uranyl secondary minerals containing the sulphate anion as reported by Čejka show that bands in the SO_4^{2-} symmetric stretching region may be but need not be observed³⁴. Serezhkina et al. (1981) observed two bands at 1012 and 1002 cm^{-1} and attributed them to the ν_1 (SO_4)²⁻³⁵. The Raman spectrum is clearer with a sharp intense band at 1042 cm^{-1} attributed to the (SO_4)²⁻ symmetric stretching vibration. Three Raman bands are observed at 1147, 1100 and 1090 cm^{-1} and are assigned to the (SO_4)²⁻ antisymmetric stretching vibrations. In the infrared spectrum two bands are observed at 1145 and 1086 cm^{-1} . Serezhkina et al. (1982) attributed bands at 1227, 1160, 1140, 1070 and 1037 to the ν_3 SO_4^{2-} . Čejka proposes that the symmetry of the (SO_4)²⁻ anion must be of C_1 symmetry. If this is so then the ν_1 and ν_2 bands become infrared active. In this work no infrared band equivalent to the symmetric stretching mode is observed. Thus it is suggested that a higher site symmetry C_{3v} is possible. However, Serezhkina et al. (1982) assigned two bands to the ν_1 SO_4^{2-} as mentioned above.

A number of Raman bands are observed in the 1050 to 1150 cm^{-1} region and are assigned to the SO_4^{2-} antisymmetric stretching vibrations (Figure 4). Raman bands are observed at 1081, 1090.7 and 1130 cm^{-1} and shift to 1082, 1090 and 1132 cm^{-1} at 77 K. An intense Raman band is observed for zippeite at 1261 cm^{-1} which shows a slight shift to lower wavenumbers upon cooling to 77 K. One possible assignment is that this band is due to a U-OH deformation mode. Four bands were observed for uranopilite at around 1178, 1145, 1115 and 1096 cm^{-1} (Frost et al in press). These bands were ascribed the SO_4^{2-} antisymmetric stretching vibrations. A broad band is also observed for uranopilite at 1272 cm^{-1} . It is not known what the attribution of this band is due to, but one possibility is that it is assignable to U-OH deformation modes.

There are four bands observed for zippeite in the spectral profile centred upon 840

cm^{-1} at 840, 841, 833 and 823 cm^{-1} (Figure 5). These bands are assigned to the $\nu_1 (\text{UO}_2)^{2+}$ symmetric stretching vibrations. The bands show a slight shift to higher wavenumbers upon collecting the spectra at 77 K. In the infrared spectrum of zippeite (Figure 3) two low intensity bands are observed at 815 and 821 cm^{-1} and are attributed to the infrared $\nu_1 (\text{UO}_2)^{2+}$ symmetric stretching vibrations. The two infrared bands at 880 and 912 cm^{-1} are assigned to the $\nu_3 (\text{UO}_2)^{2+}$ antisymmetric stretching vibrations. No Raman bands are observed in these positions for Na zippeite. In the Raman spectrum of johannite in the 650 to 1100 cm^{-1} range at 298 K three bands are observed at 812, 788 and 756 cm^{-1} and are attributed to the ν_1 symmetric stretching modes of the $(\text{UO}_2)^{2+}$ units. In the infrared spectrum of johannite two bands are observed at 936 (as a shoulder) and 898 cm^{-1} . Čejka assigned these bands to the ν_3 antisymmetric stretching modes of the $(\text{UO}_2)^{2+}$ units²³. In the infrared spectrum a band of uranopilite is observed at 838 cm^{-1} and are ascribed to the infrared activated symmetric stretching modes. Multiple infrared bands for uranopilite are observed at 932, 912, 888 and 863 cm^{-1} . The probable assignment of these bands is to the ν_3 antisymmetric stretching modes of the $(\text{UO}_2)^{2+}$ units, although there may be also a coincidence of the uranyl stretching vibrations bands and those of δ U-OH bending bands.

U-O bond lengths in uranyles may be calculated with the empirical relations by Bartlett and Cooney³⁶. Raman bands, observed in sample No.1 at $886.6 \text{ cm}^{-1}/1.794 \text{ \AA}$ (298 K) and $888.6 \text{ cm}^{-1}/1.793 \text{ \AA}$ (77 K) (IR bands $926.9 \text{ cm}^{-1}/1.765 \text{ \AA}$; $908.7 \text{ cm}^{-1}/1.778 \text{ \AA}$; $894.2 \text{ cm}^{-1}/1.789 \text{ \AA}$; $884.7 \text{ cm}^{-1}/1.796 \text{ \AA}$; $877.6 \text{ cm}^{-1}/1.801 \text{ \AA}$; $856.9 \text{ cm}^{-1}/1.817 \text{ \AA}$) and in sample No. 2 at $887 \text{ cm}^{-1}/1.794 \text{ \AA}$ (298 K) and at $924.2 \text{ cm}^{-1}/1.767 \text{ \AA}$; $896.6 \text{ cm}^{-1}/1.787 \text{ \AA}$; $888.6 \text{ cm}^{-1}/1.793 \text{ \AA}$; $869.8 \text{ cm}^{-1}/1.807 \text{ \AA}$; $858.6 \text{ cm}^{-1}/1.816 \text{ \AA}$ (77 K) (IR bands $926.2 \text{ cm}^{-1}/1.766 \text{ \AA}$; $912 \text{ cm}^{-1}/1.776 \text{ \AA}$; $880.4 \text{ cm}^{-1}/1.799 \text{ \AA}$; $858 \text{ cm}^{-1}/1.816 \text{ \AA}$) are attributed to the $\nu_3 (\text{UO}_2)^{2+}$ antisymmetric stretching vibrations. Raman bands in sample No. 1 at $841.4 \text{ cm}^{-1}/1.770 \text{ \AA}$; $839.8 \text{ cm}^{-1}/1.771 \text{ \AA}$; $833.5 \text{ cm}^{-1}/1.777 \text{ \AA}$; $823.3 \text{ cm}^{-1}/1.787 \text{ \AA}$; $813.3 \text{ cm}^{-1}/1.797 \text{ \AA}$ (298 K) and at $844 \text{ cm}^{-1}/1.767 \text{ \AA}$; $843.4 \text{ cm}^{-1}/1.768 \text{ \AA}$; $838.3 \text{ cm}^{-1}/1.773 \text{ \AA}$; $828.2 \text{ cm}^{-1}/1.783 \text{ \AA}$; $823.4 \text{ cm}^{-1}/1.787 \text{ \AA}$; $813.5 \text{ cm}^{-1}/1.797 \text{ \AA}$; $803.1 \text{ cm}^{-1}/1.808 \text{ \AA}$ (298 K) (IR bands at $844.8 \text{ cm}^{-1}/1.767 \text{ \AA}$; $820.9 \text{ cm}^{-1}/1.790 \text{ \AA}$; $801.6 \text{ cm}^{-1}/1.809 \text{ \AA}$; $794 \text{ cm}^{-1}/1.817 \text{ \AA}$) and in sample No. 2 $841.5 \text{ cm}^{-1}/1.770 \text{ \AA}$; $839.8 \text{ cm}^{-1}/1.771 \text{ \AA}$; $832.8 \text{ cm}^{-1}/1.778 \text{ \AA}$; $824.8 \text{ cm}^{-1}/1.786 \text{ \AA}$; $812.9 \text{ cm}^{-1}/1.798 \text{ \AA}$; $807.7 \text{ cm}^{-1}/1.803 \text{ \AA}$) are assigned to the $\nu_1 (\text{UO}_2)^{2+}$ symmetric stretching vibrations. U-O bond lengths calculated with two empirical relations³⁶ are in agreement with those from the single crystal structure data $\approx 1.77 \text{ \AA}$ ¹⁴. An overlap / a coincidence of the $(\text{UO}_2)^{2+}$ stretching vibrations and δ U-OH bending vibrations may be expected and cannot be excluded. Raman and especially infrared bands connected with δ U-OH bending vibrations are observed also in the region 1560 - 1300 cm^{-1} (Figure 4).

Bands in the region $560 - 350 \text{ cm}^{-1}$ mostly connected with the $(\text{SO}_4)^{2-}$ bending vibrations are discussed below. However, some of the Raman bands in the range 560 - 440 cm^{-1} may be attributed to the ν (bridge elongation) (U_3O) , 390 - 350 cm^{-1} to the ν (group elongation) $\text{U}_3(\text{OH})_3$, 340 - 270 to the γ (out-of-plane bending) (U_3O) , and 230 - 210 cm^{-1} to the γ (out-of-plane bending) and δ (in-plane bending) $\text{U}_3(\text{OH})_3$. The presence of such units may be predicted from the structure of synthetic sodium-zippeite. Bands observed at lower wavenumbers than approximately 210 cm^{-1} are related to lattice vibrations and translations. The Raman spectrum of the low wavenumber region of zippeite at 298 and 77 K are shown in Figure 6. A band is observed at 669 cm^{-1} at 298 K and is assigned to the triply degenerate ν_4 bending vibration of the $(\text{SO}_4)^{2-}$ units. This band is found at 672 cm^{-1} at 77 K. No additional bands were resolved at this temperature in this spectral region. In the infrared spectrum two absorption bands are observed at 619 and 605 cm^{-1} and may be assigned to this vibrational mode. Čejka found absorption band at 619 cm^{-1} which is in good agreement with this work²³,

and Serezhkina et al. found four bands at 642, 611, 605 and 595 cm^{-1} for johannite assigned to the $\nu_4 (\text{SO}_4)^{2-}$.

Intense bands are observed in the 373 to 497 cm^{-1} region and are attributed to the ν_2 bending modes of the $(\text{SO}_4)^{2-}$ units. The observation of more than one band in this spectral region suggests a lowering of the symmetry of the sulphate anion to C_{3v} or less. Bands in the 398 cm^{-1} region are assigned to the $\nu_2 \text{SO}_4^{2-}$ bending vibrations. Some bands may be also related to the $\nu \text{U-O}_{\text{equatorial}}$, i.e. $\text{U-O}_{\text{ligand}}$ vibrations³⁷. Intense bands observed in the Raman spectra at 77 K are also connected with these $\nu_2 \text{SO}_4^{2-}$ bending vibrations. Bands at wavenumbers lower than 320 cm^{-1} observed in the Raman spectra (Fig. 6) - not measured in the infrared spectra, are attributed to the $\nu_2 (\delta) \text{UO}_2^{2+}$ bending vibrations and the lowest bands (180-260 cm^{-1}) may be assigned to the lattice and/or $\text{O}_l\text{-U-O}_{\text{ligand}}$ vibrations³⁸ and /or cation and anion librations³⁹. In each of the spectra bands are observed at around 322, 294, 260 cm^{-1} . Any unambiguous assignment of bands in this range is very complex.

In the 298 K spectrum for johannite Frost et al found three bands are observed at 302, 277 and 205 cm^{-1} . In the 77 K spectrum, bands shifted to 306, 282, 231 and 210 cm^{-1} with other low intensity bands found at 191, 170 and 149 cm^{-1} . In the infrared spectrum of johannite Čejka assigned the two bands at 257 and 216 cm^{-1} to the doubly degenerate ν_2 bending vibration of the $(\text{UO}_2)^{2+}$ units.

OH stretching region

In the crystal structure of sodium-zippeite, there are three symmetrically distinct hydroxyls in the uranyl anion sheet, and twelve water molecules in the interlayer¹⁴. Water molecules are coordinated to Na^+ -cations and participate together with the sheet hydroxyls in formation of hydrogen-bonding network. This hydrogen-bonding network influences origin and formation of the crystal structure of sodium-zippeite and plays an important role in the stability of this natural phase⁴⁰⁻⁴². Infrared bands in the range 3600-2800 cm^{-1} are attributed to the ν OH stretching vibrations of water molecules and hydroxyls without any possible resolution the ν_1 and ν_3 (Figure 7). Libowitzky's empirical relation enables to infer the O-H...O bond lengths from the wavenumbers of the observed tops of bands⁴³. These lengths ($\text{cm}^{-1}/\text{\AA}$) are for sample No.1 3600/>3.2; 3558.6/3.04; 3504.2/2.902; 3475.7/2873; 3455.9/2853; 3302.4/2.75; 3079.1/2.676; 2876.8/2.63 and for sample No. 2 3600/>3.2; 3559.3/3.042; 3505.2/2.905; 3456.1/2853; 3452.1/2.85; 3281.1/2.74; 3127.4/2.687.

From the observed and calculated data may be inferred that there are free or very weakly bonded three $(\text{OH})^-$ units in the structure of both sodium-zippeite samples. This is in agreement with the structure¹⁴. Deconvolution of broad bands enables to prove the presence of strongly hydrogen bonded water molecules¹⁴. Uranyl oxygen and some other uranyl anion sheet oxygens and hydroxyls may participate in the formation and arrangement of the hydrogen-bonding network with water molecules from the interlayer. Hydrogen bonding between water molecules in the interlayer is also supposed. According to Hawthorne⁴⁴, a complex crystal structure may be understood as composed of two units - strongly bonded structural units - uranyl anion sheets, and the weakly bonded interstitial complex - the interlayer. The bonding interaction between the structural unit and the interstitial complex is weak. This weak interaction controls the stability of the structure⁴⁴.

A set of 5 bands (1645.7; 1628.8; 1625.2; 1618.6 cm^{-1}) for sample No. 1 and of 3 bands (1646.3; 1627.8; 1619.7 cm^{-1}) may be assigned to the $\delta \text{H}_2\text{O}$ bending vibrations (Figure 8). Only bands at 1612.9 cm^{-1} (298 K) and 1675.3 cm^{-1} (77 K) were observed in the Raman

spectra of sample No. 2. Raman and infrared spectroscopy study of sodium-zippeite confirms that structurally nonequivalent water molecules are present in its structure. This is in agreement with the structure¹⁴ and thermal analysis²³ of synthetic sodium-zippeite.

Conclusions

- (a) Raman and infrared spectra of two samples of sodium-zippeite from Happy Jack Mine were studied.
- (b) Bands connected with the $(\text{UO}_2)^{2+}$ and $(\text{SO}_4)^{2-}$ stretching and bending vibrations were attributed respecting their number as a result of FGA-correlation.
- (c) Coincidence of some of these bands with the bands assigned to U-OH bending vibrations is probable.
- (d) U-O bond lengths in uranyls were calculated and compared with the X-ray single crystal structure data. Both data are in good agreement.
- (e) Three free or very weak hydrogen bonded symmetrically distinct hydroxyls located in the sheets were inferred from the spectra. This agrees with the structure of sodium-zippeite.
- (f) Water molecules of the interlayer participate in a set of hydrogen bonds forming thus a complex hydrogen-bonding network which influences the origin, formation and stability of the mineral.
- (g) Relatively large interlayer probably enables introducing of mono- and/or divalent-cations and water molecules influencing thus possible existence of solid solutions² and mineral stability by hydrogen-bonding network^{40,41,44}.

References

1. Finch, R, Murakami, T. *Reviews in Mineralogy* 1999; **38**: 91.
2. McCollam, BE. University of Notre Dame 2004.
3. Frondel, C *Systematic Mineralogy of Uranium and Thorium*, 1958.
4. Frondel, C, Weeks, AD. *Proc. UN Intern. Conf. Peaceful Uses Atomic Energy, 2nd, Geneva, 1958* 1958; **2**: 277.
5. Frondel, C, Ito, J, Honea, RM, Weeks, AM. *Canadian Mineralogist* 1976; **14**: 429.
6. Frost, RL, Cejka, J, Weier, M, Ayoko, GA. *Journal of Raman Spectroscopy* 2006; **37**: 1362.
7. Frost, RL, Cejka, J, Weier, M, Martens, WN. *Journal of Raman Spectroscopy* 2006; **37**: 879.
8. Frost, RL, Cejka, J, Weier, ML, Martens, W. *Journal of Raman Spectroscopy* 2006; **37**: 538.
9. Frost, RL, Weier, ML, Cejka, J, Kloprogge, JT. *Journal of Raman Spectroscopy* 2006; **37**: 585.
10. Frost, RL, Weier, ML, Reddy, BJ, Cejka, J. *Journal of Raman Spectroscopy* 2006; **37**: 816.
11. Frost, RL, Henry, DA, Erickson, K. *Journal of Raman Spectroscopy* 2004; **35**: 255.
12. O'Brien, TJ, Williams, PA. *Inorganic and Nuclear Chemistry Letters* 1981; **17**: 105.
13. Haacke, DF, Williams, PA. *Mineralogical Magazine* 1979; **43**: 539.
14. Burns, PC, Deely, KM, Hayden, LA. *Canadian Mineralogist* 2003; **41**: 687.
15. Burns, PC. *Can. Mineral* 2005; **43**: 1839.
16. Burns, PC, Ewing, RC, Hawthorne, FC. *Canadian Mineralogist* 1997; **35**: 1551.
17. Burns, PC, Miller, ML, Ewing, RC. *Canadian Mineralogist* 1996; **34**: 845.
18. Ondrus, P, Veselovsky, F, Hlousek, J, Skala, R, Vavrin, I, Fryda, J, Cejka, J, Gabasova, A. *Journal of the Czech Geological Society* 1997; **42**: 3.
19. Elton, NJ, Hooper, JJ. *Mineralogical Magazine* 1993; **57**: 352.
20. Paulis, P, Sikola, D, Holeczy, D. *Vestnik Ceskeho Geologickeho Ustavu* 1994; **69**: 87.
21. Meisser, N. 2003.
22. Sejkora, J, Cejka, J, Škácha, P, Gabašová, A, Novotná, M. *Bull. mineral.-petrolog. Odd. Nár. Muz (Praha)* 2003; **11**: 183.
23. Cejka, J. *Reviews in Mineralogy* 1999; **38**: 521.
24. Frost, RL, Palmer, SJ, Bouzaid, JM, Reddy, BJ. *Journal of Raman Spectroscopy* 2007; **38**: 68.
25. Frost, RL, Henry, DA, Weier, ML, Martens, W. *Journal of Raman Spectroscopy* 2006; **37**: 722.
26. Frost, RL, Musumeci, AW, Kloprogge, JT, Adebajo, MO, Martens, WN. *Journal of Raman Spectroscopy* 2006; **37**: 733.
27. Frost, RL, Weier, ML, Martens, WN, Kloprogge, JT, Kristof, J. *Journal of Raman Spectroscopy* 2005; **36**: 797.
28. Frost, RL, Wills, R-A, Weier, ML, Martens, W. *Journal of Raman Spectroscopy* 2005; **36**: 435.
29. Frost, RL, Weier, ML. *Thermochimica Acta* 2003; **406**: 221.
30. Frost, RL, Weier, ML, Kloprogge, JT. *Journal of Raman Spectroscopy* 2003; **34**: 760.
31. Frost, RL, Weier, ML. *Journal of Raman Spectroscopy* 2003; **34**: 776.
32. Frost, RL, Weier, ML. *Thermochimica Acta* 2004; **409**: 79.
33. Gaines, RV, Skinner, HCW, Foord, EE, Mason, B, Rosenzweig, A *Dana's new mineralogy*, 8th ed.; John Wiley and Sons: New York, 1997.
34. Cejka, J, Urbanec, Z, Cejka, J, Jr., Mrazek, Z. *Neues Jahrbuch fuer Mineralogie, Abhandlungen* 1988; **159**: 297.
35. Serezhkin, VN. *Geokhimiya* 1981: 1677.
36. Bartlett, JR, Cooney, RP. *Journal of Molecular Structure* 1989; **193**: 295.
37. Hoekstra, HR, Siegel, S. *Journal of Inorganic and Nuclear Chemistry* 1973; **35**: 761.
38. Volod'ko, LV, Komyak, AI, Umreiko, DS *Uranyl Compounds, Vol. 1: Spectra, Structure*, 1981.
39. Anderson, A, Chieh, C, Irish, DE, Tong, JPK. *Canadian Journal of Chemistry* 1980; **58**: 1651.
40. Hawthorne, FC. *Zeitschrift fuer Kristallographie* 1992; **201**: 183.
41. Hawthorne, FC. *Acta Crystallographica, Section B: Structural Science* 1994; **B50**: 481.
42. Hawthorne, FC. *EMU Notes in Mineralogy I* 1997; **European Mineralogical Union**: 373.
43. Libowitzky, E. *Monatshefte fuer Chemie* 1999; **130**: 1047.
44. Hawthorne, FC. *Geologiya Rudnykh Mestorozhdenii* 2003; **45**: 100.

Table 1. Elemental concentrations in weight % from EDX analyses of crystal clusters from the zippeite sample from Happy Jack Mine, USA. Oxygen was calculated indirectly by stoichiometry.

Wt %	C	O	U	S	Na	Total
1		19.73	76.21	1.99	2.07	100.00
2		8.94	89.08	1.25	0.73	100.00
3		21.72	74.78	2.65	0.84	99.99
4	11.16	25.96	52.53	2.99	5.11	100.00
4'	-	34.85	59.13	3.36	2.66	100.00
5		3.05	95.03	1.92	0	100.00

ν_3 cm^{-1}	IR	Raman 298 K	Raman 298 K	Raman 77 K
	890.1	888.2	880.7	864.4
	1.773 Å	1.775 Å	1.779 Å	1.790 Å
³⁶	1.792 Å	1.793 Å	1.799 Å	1.811 Å
	1.787 Å	1.788 Å	1.792 Å	1.802 Å
ν_1 cm^{-1}	IR	Raman 298 K	Raman 298 K	Raman 77 K
	850.4/798.6	845.7/827.3/810.2	841.1/830.4	812.9
³⁶	1.761 Å 1.812 Å	1.766 Å 1.783 Å 1.800 Å	1.770 Å 1.780 Å	1.790 Å

Table 2 Comparison of the bond lengths as calculated from the ν_1 and ν_3 band positions

List of Figures

Figure 1 SEM image of sodium zippeite from the Happy Jack Mine. (The numeric indicates an example of the the position of the EDX analyses)

Figure 2 Raman spectra of sodium zippeite in the 950 to 1050 cm^{-1} region at 298 and 77 K.

Figure 3 Infrared spectra of sodium zippeite in the 500 to 1300 cm^{-1} region

Figure 4 Raman spectra of sodium zippeite in the 1050 to 1450 cm^{-1} region at 298 and 77 K.

Figure 5 Raman spectra of sodium zippeite in the 750 to 950 cm^{-1} region at 298 and 77 K.

Figure 6 Raman spectra of sodium zippeite in the 150 to 750 cm^{-1} region at 298 and 77 K.

Figure 7 Infrared spectra of sodium zippeite in the 2550 to 3700 cm^{-1} region

Figure 8 Infrared spectra of sodium zippeite in the 1400 to 1800 cm^{-1} region

List of Tables

Table 1. Elemental concentrations in weight % from EDX analyses of crystal clusters from the zippeite sample from Happy Jack Mine, USA. Oxygen was calculated indirectly by stoichiometry.

Table 2 Comparison of the bond lengths as calculated from the ν_1 and ν_3 band positions

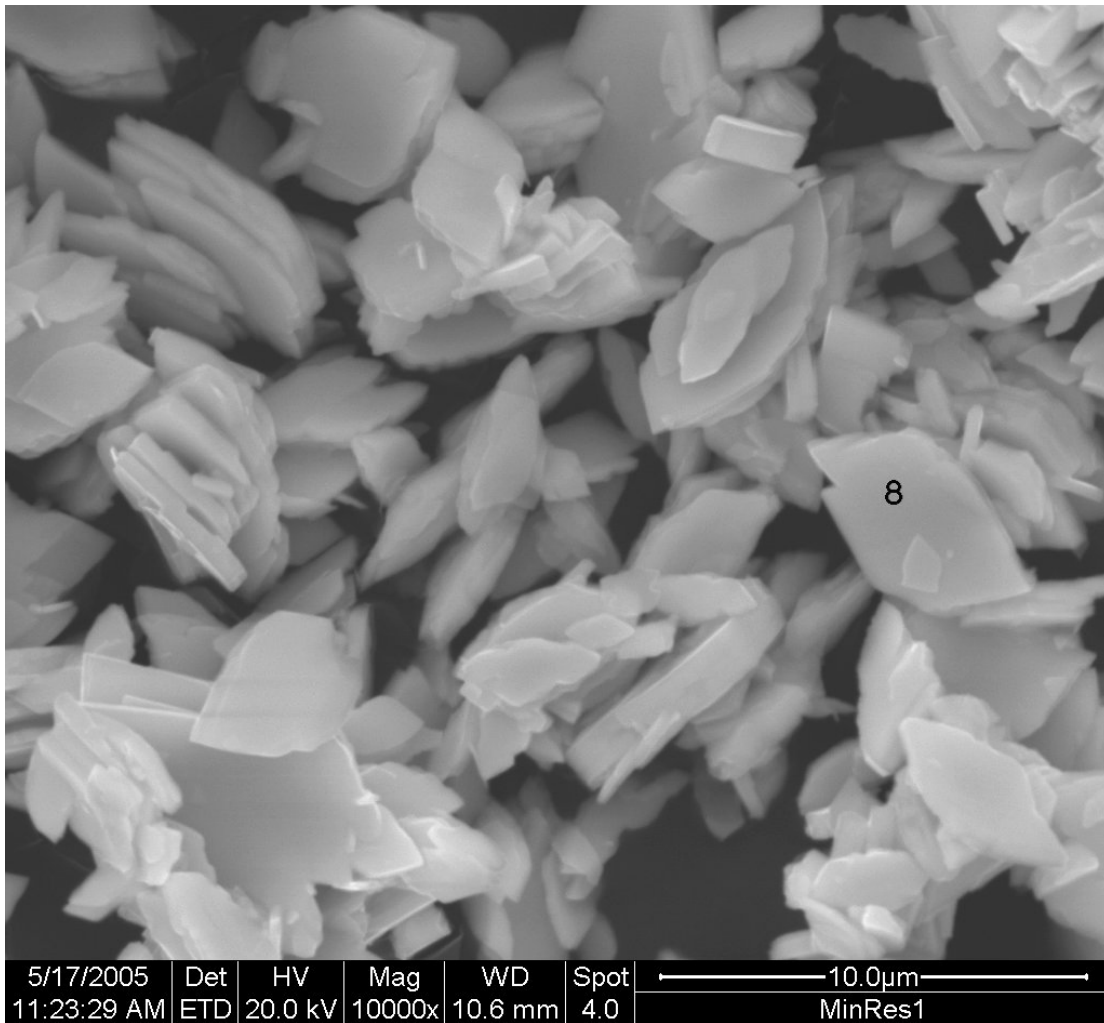


Figure 1

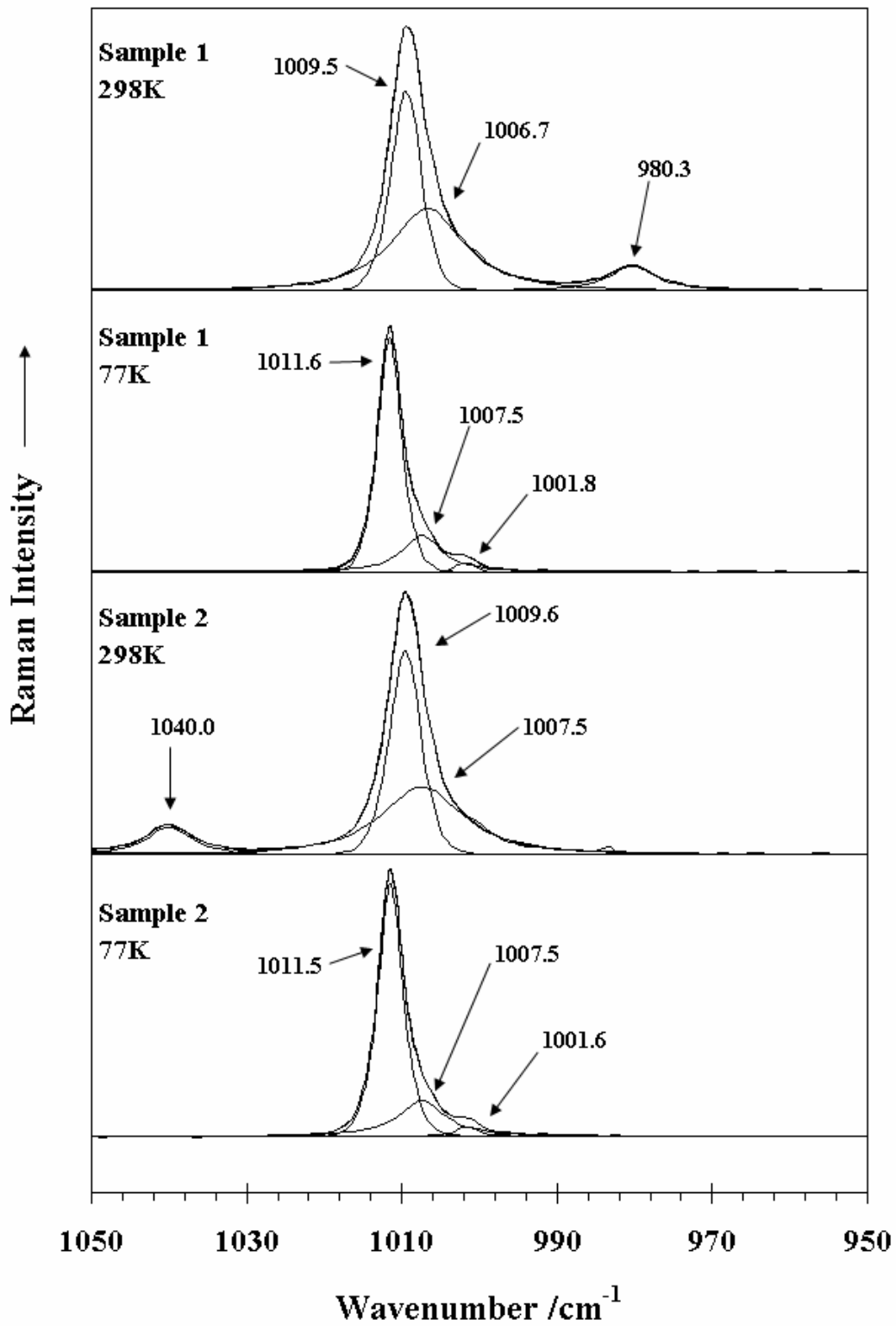


Figure 2

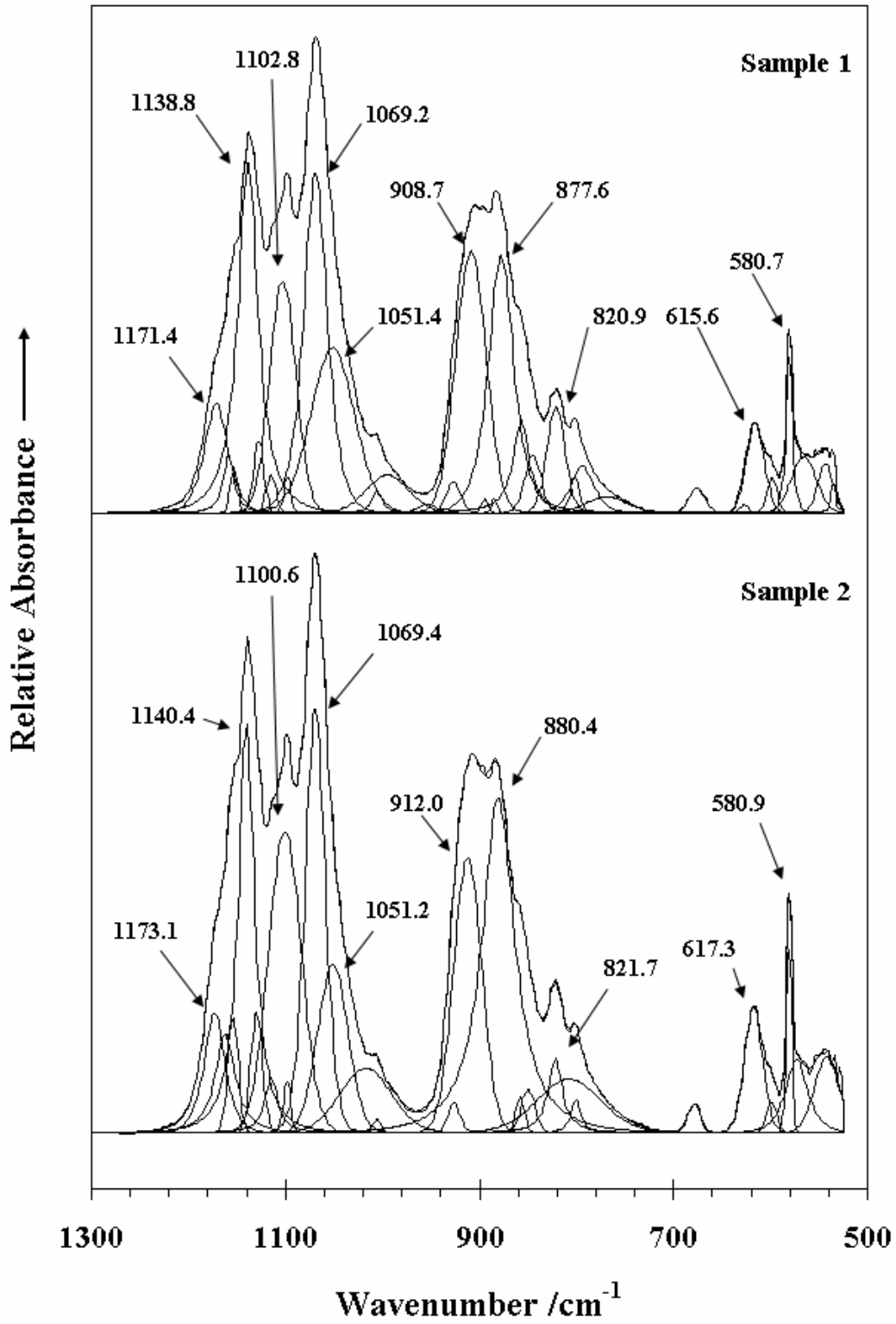


Figure 3

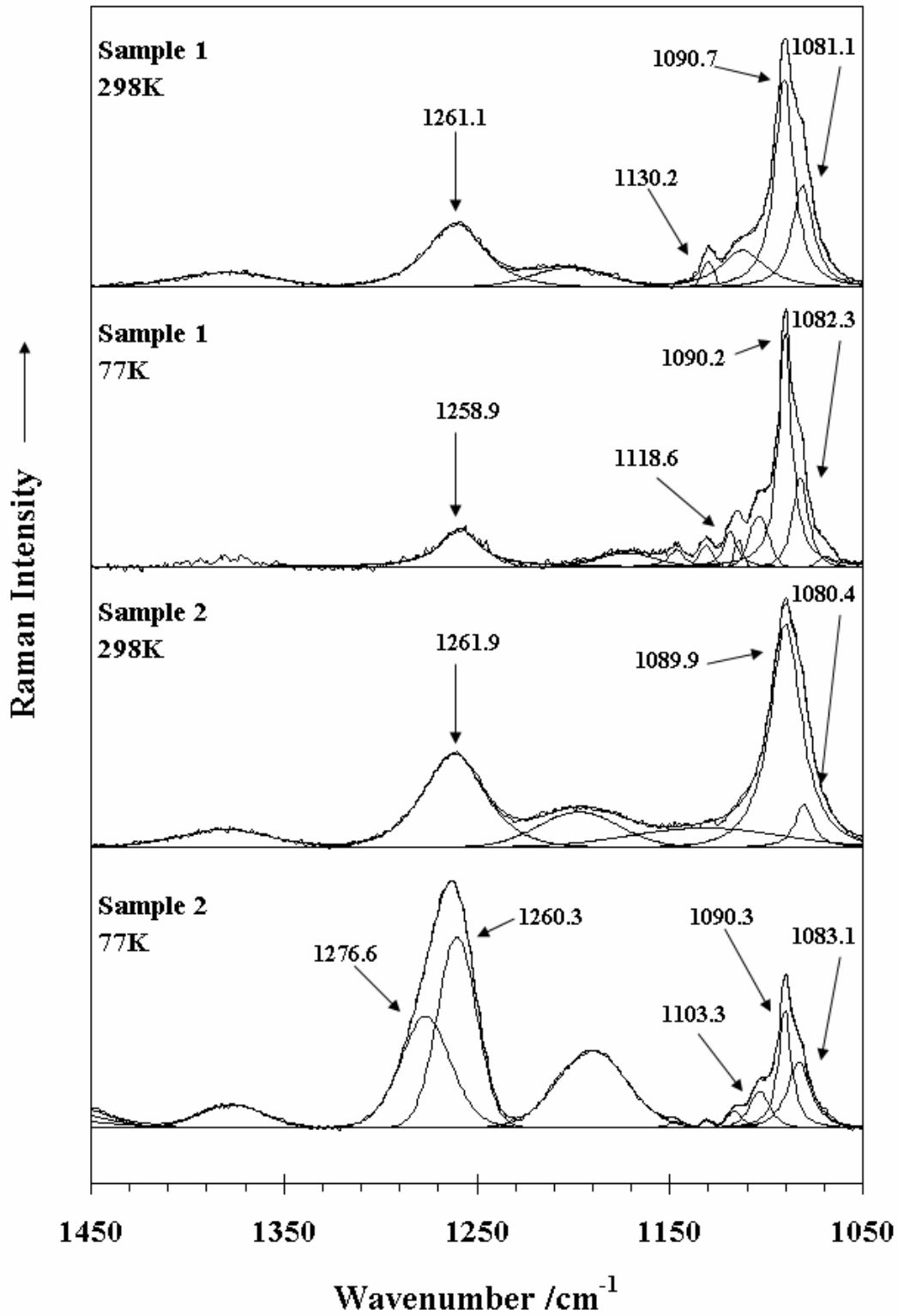


Figure 4

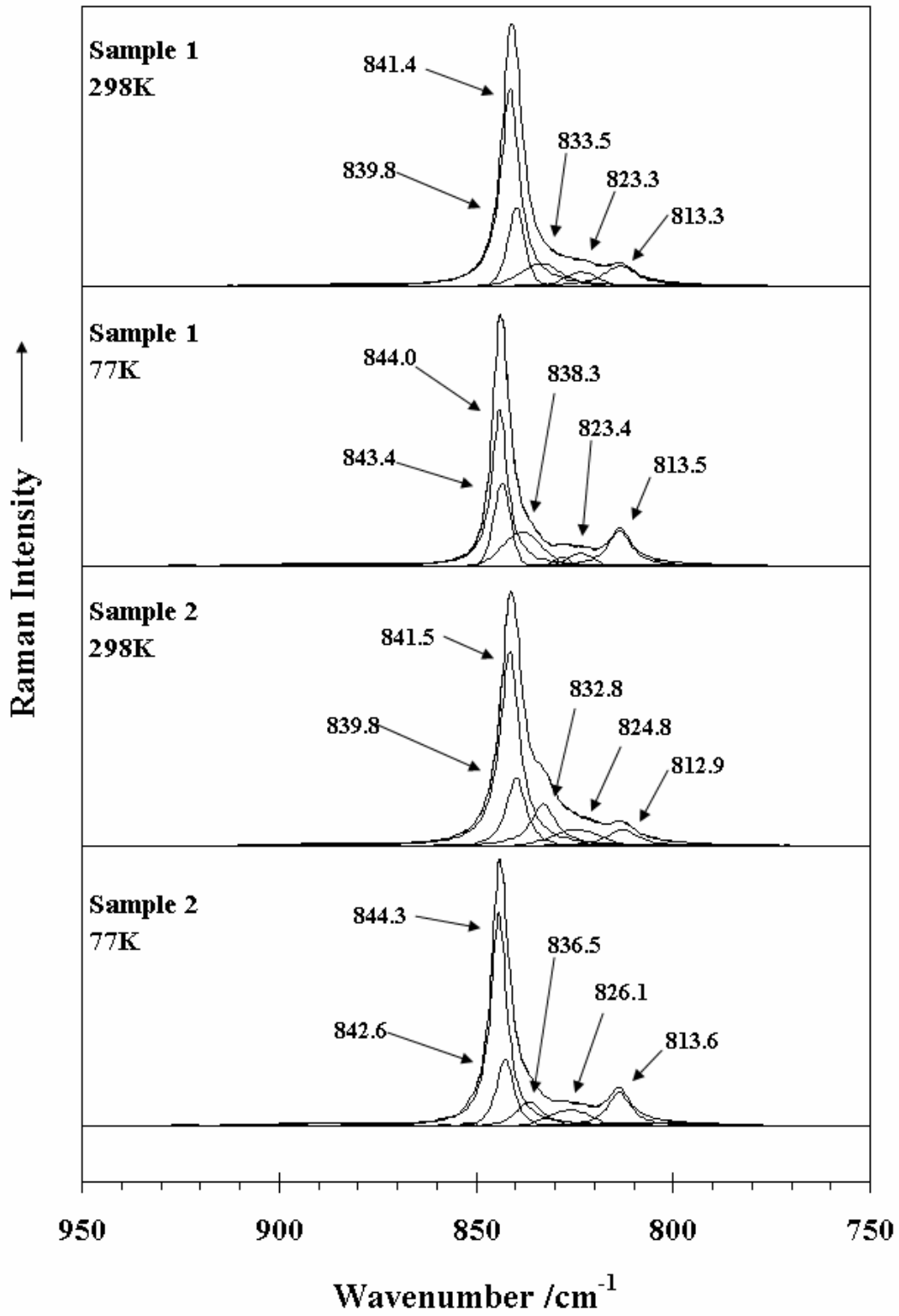


Figure 5

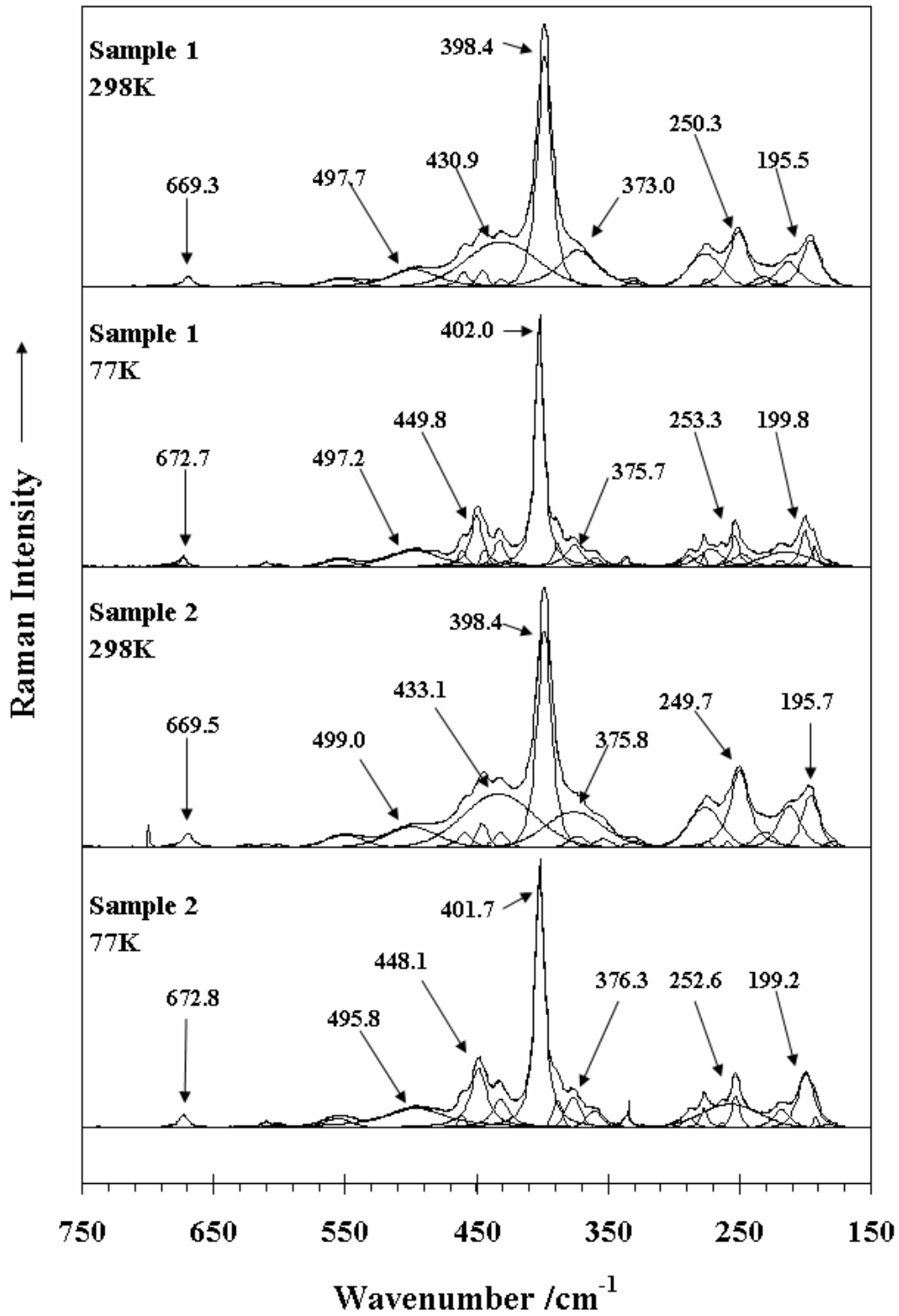


Figure 6

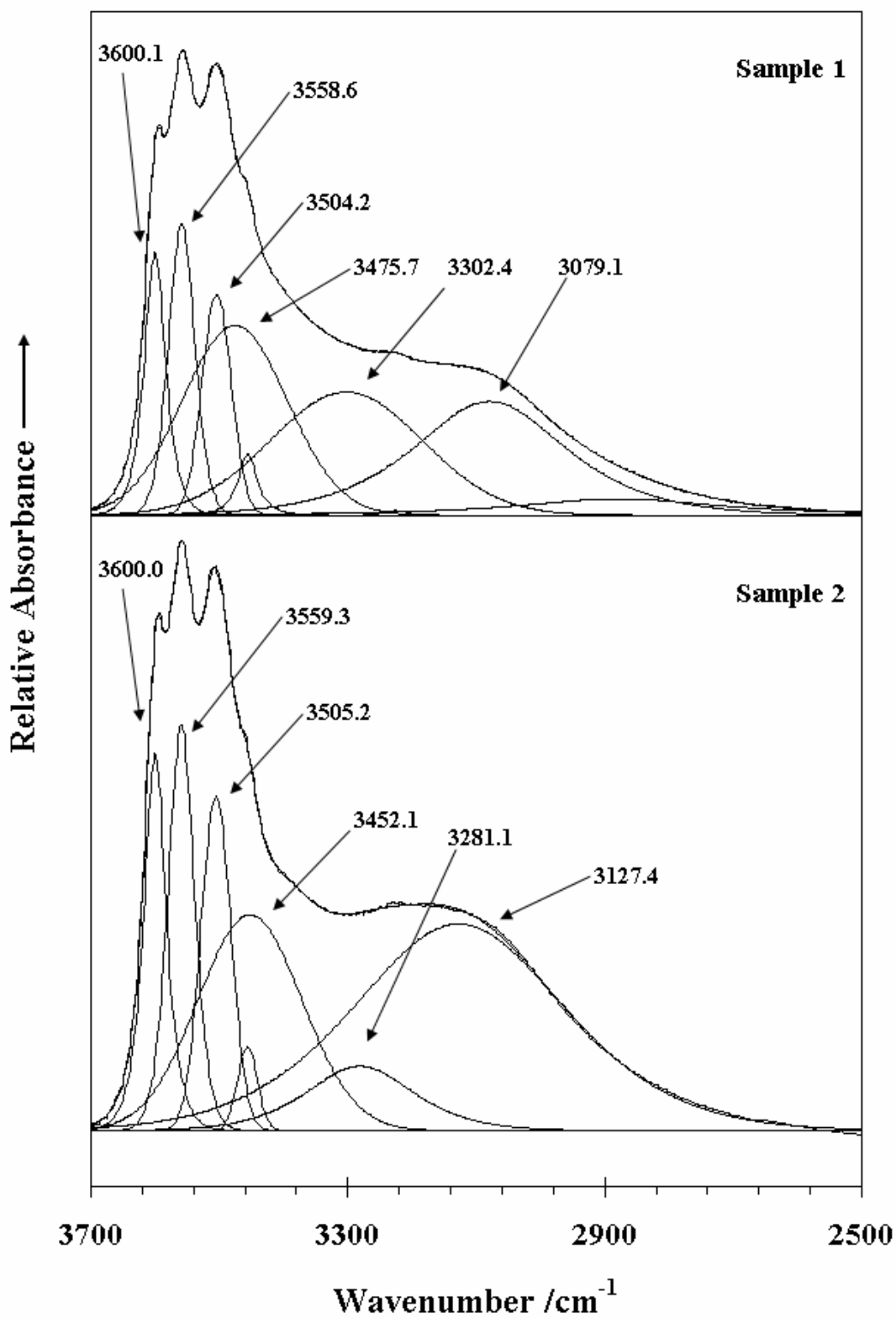


Figure 7

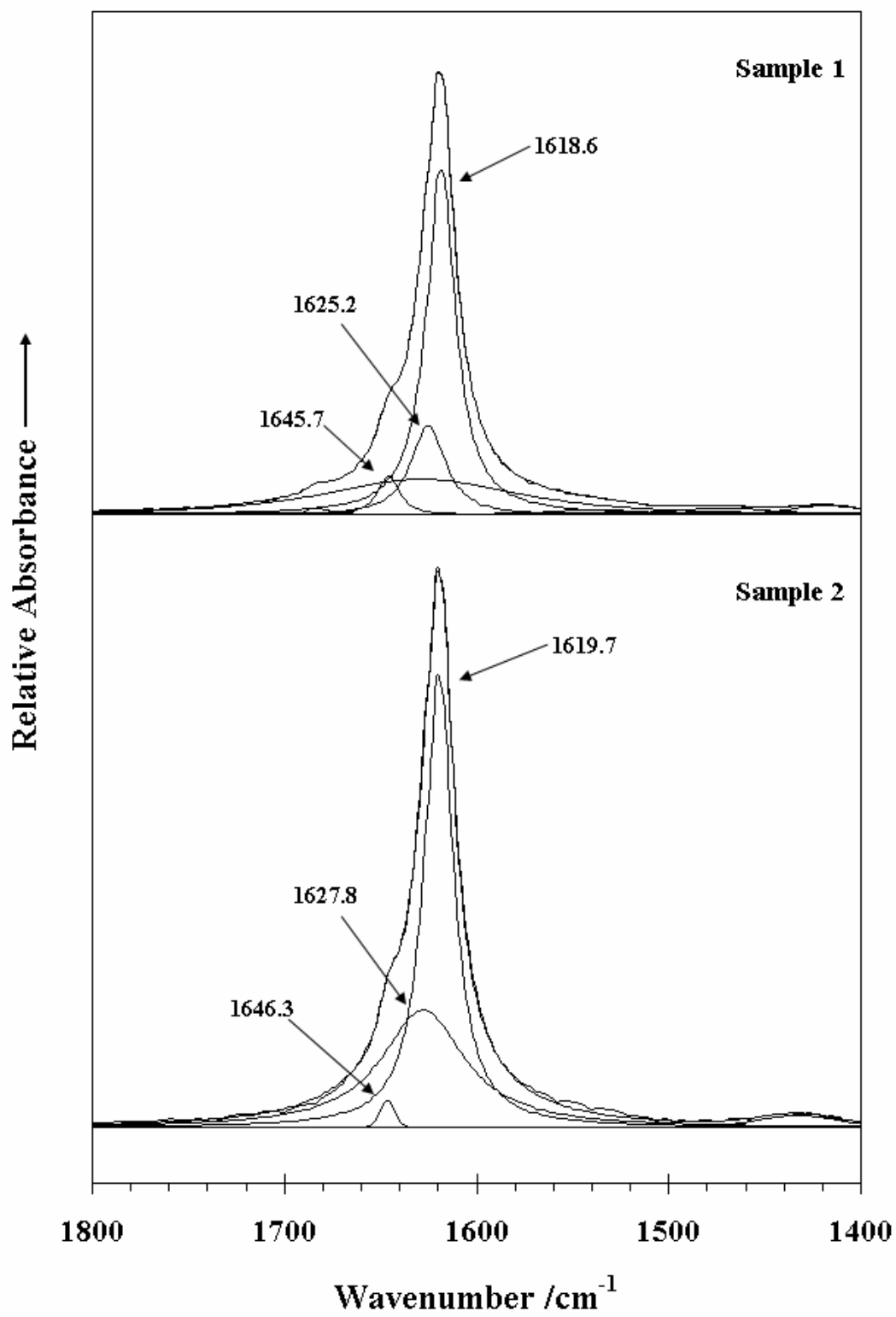


Figure 8

